AD-A177 993 INVESTIGATION OF TEARING INSTABILITY PHENOMENA IN ASTM 1/1
STEEL(U) DAVID W TAYLOR NAVAL SHIP RESEARCH AND
DEVELOPMENT CENTER ANN. R E LINK ET AL. NOV 86
UNCLASSIFIED DTNSRDC/SME-86-31 F/G 11/6 NL

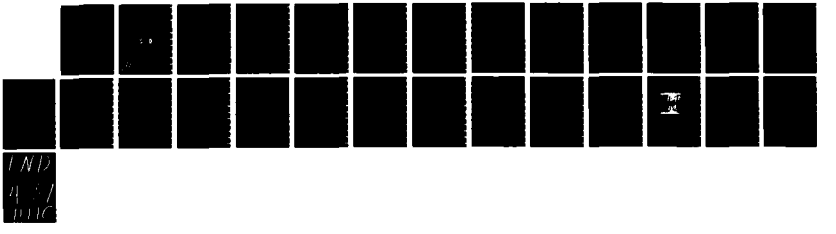

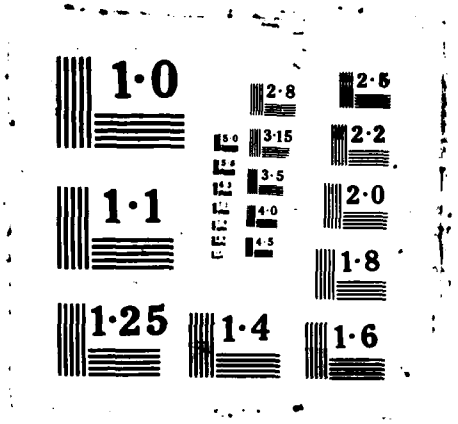
1·0
1·1
1·25
2·8
3·15
3·5
4·0
4·5
1·4
2·5
2·2
2·0
1·8
1·6

(12)

David W. Taylor Naval Ship Research and Development Center

Bethesda, MD 20084-5000

DTNSRDC/SME-86-31 November 1986

Ship Materials Engineering Department

Research and Development Report

INVESTIGATION OF TEARING INSTABILITY PHENOMENA IN ASTM A106 STEEL

by

Richard E. Link

Richard A. Hays

DTNSRDC/SME-86-31 INVESTIGATION OF TEARING INSTABILITY PHENOMENA IN ASTM A106 STEEL

UNCLASSIFIED
SECURITY CLASSIFICATION OF THIS PAGE

AD-A177993

REPORT DOCUMENTATION PAGE

1a REPORT SECURITY CLASSIFICATION UNCLASSIFIED	1b RESTRICTIVE MARKINGS
2a SECURITY CLASSIFICATION AUTHORITY	3 DISTRIBUTION / AVAILABILITY OF REPORT Approved for public release; distribution unlimited.
2b DECLASSIFICATION / DOWNGRADING SCHEDULE	
4 PERFORMING ORGANIZATION REPORT NUMBER(S) DTNSRDC/SME-86-31	5 MONITORING ORGANIZATION REPORT NUMBER(S)
6a NAME OF PERFORMING ORGANIZATION DTNSRDC 6b OFFICE SYMBOL (If applicable) Code 2814	7a NAME OF MONITORING ORGANIZATION
6c ADDRESS (City, State, and ZIP Code) Bethesda, MD 20084-5000	7b ADDRESS (City, State, and ZIP Code)
8a NAME OF FUNDING / SPONSORING ORGANIZATION U.S. Nuclear Regulatory Comm. 8b OFFICE SYMBOL (If applicable)	9 PROCUREMENT INSTRUMENT IDENTIFICATION NUMBER
8c ADDRESS (City, State, and ZIP Code) Washington, DC 20555	10 SOURCE OF FUNDING NUMBERS PROGRAM ELEMENT NO / PROJECT NO / TASK NO / WORK UNIT ACCESSION NO 1-2814-553

11 TITLE (Include Security Classification)

(U) INVESTIGATION OF TEARING INSTABILITY PHENOMENA IN ASTM A106 STEEL

12 PERSONAL AUTHOR(S)
R.E. Link, R.A. Hays

13a TYPE OF REPORT	13b TIME COVERED	14 DATE OF REPORT (Year, Month, Day)	15 PAGE COUNT
Final	FROM _____ TO _____	November 1986	27

16 SUPPLEMENTARY NOTATION

Prepared under Interagency Agreement RES-78-104

17 COSATI CODES			18 SUBJECT TERMS (Continue on reverse if necessary and identify by block number)
FIELD	GROUP	SUB-GROUP	
			J-integral, tearing instability, ASTM A106 steel, steel

19 ABSTRACT (Continue on reverse if necessary and identify by block number)

An experimental investigation was performed to evaluate tearing instability theory by varying the applied tearing modulus, $T_{applied}$, so that fracture instability would be initiated at various levels of stable crack extension. This is an extension of past investigations of tearing instability theory in that crack extension was monitored continuously using the D.C. potential drop technique, enabling the applied and material tearing moduli to be calculated at the point of instability.

The results of this investigation indicate that, in most cases, fracture instability occurred when the difference between the applied and material tearing moduli was on the order of 10%. Variations in the load versus displacement records of the specimens near maximum load due to local instabilities and friction in the load train precluded measurement of a smooth applied tearing modulus curve.

20 DISTRIBUTION / AVAILABILITY OF ABSTRACT	21 ABSTRACT SECURITY CLASSIFICATION
☐ UNCLASSIFIED/UNLIMITED ☒ SAME AS RPT ☐ DTIC USERS	UNCLASSIFIED
22a NAME OF RESPONSIBLE INDIVIDUAL R.E. Link	22b TELEPHONE (Include Area Code) (301) 267-4335
	22c OFFICE SYMBOL Code 2814

DD FORM 1473, 84 MAR 83 APR edition may be used until exhausted
All other editions are obsolete

SECURITY CLASSIFICATION OF THIS PAGE

☆U.S. Government Printing Office: 1985—639-012

CONTENTS

FIGURES

FIGURES (Continued)

TABLES

ABBREVIATIONS

a	crack length
ASTM	American Society for Testing and Materials
D.C.	direct current
J	joule
J-R	J-Integral resistance
ksi	thousand pound per square inch
MPa	megapascal
s	seconds
$T_{applied}$	applied tearing modulus
$T_{material}$	material tearing modulus
W	specimen width
wt %	weight percent

ABSTRACT

An experimental investigation was performed to evaluate tearing instability theory by varying the applied tearing modulus, $T_{applied}$, so that fracture instability would be initiated at various levels of stable crack extension. This is an extension of past investigations of tearing instability theory in that crack extension was monitored continuously using the D.C. potential drop technique, enabling the applied and material tearing moduli to be calculated at the point of instability.

The results of this investigation indicate that, in most cases, fracture instability occurred when the difference between the applied and material tearing moduli was on the order of 10%. Variations in the load versus displacement records of the specimens near maximum load due to local instabilities and friction in the load train precluded measurement of a smooth applied tearing modulus curve.

ADMINISTRATIVE INFORMATION

This study was sponsored by the U.S. Nuclear Regulatory Commission and was performed under Interagency Agreement RES-78-104, Modification 8. Mr. Milton Vagins and Mr. Michael Mayfield of the Materials Engineering Branch, Office of Nuclear Regulatory Research have been program technical monitors during the course of this research.

ACKNOWLEDGEMENTS

The authors gratefully acknowledge the support of the U.S. Nuclear Regulatory Commission and Mr. Milton Vagins. We would also like to thank Dr. James Joyce, Mr. Michael Vassilaros and Dr. John Gudas for their many helpful comments and suggestions.

INTRODUCTION

The tearing instability concept was developed by Paris[1] as a means of assessing the stability of flawed structures that fail by ductile tearing. Tearing instability theory states that a flawed structure loaded beyond J_{Ic} and at limit load will tear in a stable manner so long as the applied tearing modulus, $T_{applied}$, is less than the material tearing modulus, $T_{material}$. Tearing will proceed in an unstable manner whenever the $T_{applied}$ equals or exceeds $T_{material}$. Several experimental investigations were conducted to validate tearing instability theory for materials exhibiting both high and low toughness [2-4]. Vassilaros, et al.[4] used the compact tension specimen in a variably compliant screw-driven test machine to validate the tearing instability concept for several high toughness alloys with $T_{material}$ spanning the range of 12 to 170. The $T_{applied}$ formulations used to analyze the test data included the generalized expression of Paris, et al.[1], a modified Paris formulation, and an expression developed by Ernst, et al.[5] using the key curve approach. Among the conclusions of the investigation were that the $T_{applied}$ expression of Paris, et al. was non-conservative in predicting the point of instability in the compact specimen and that the generalized Paris analysis evaluated at maximum load was most consistent in predicting instability. They also concluded that the analysis of Ernst, et al. appeared to be accurate, but the analysis required precision beyond that which was available in their test data.

The purpose of the present investigation was an extension of the Vassilaros, et al.[4] study to further evaluate tearing instability theory by varying $T_{applied}$ so that instability would be initiated at various levels of

stable crack extension and to employ the Ernst analysis[5] to calculate $T_{applied}$.

EXPERIMENTAL PROCEDURE

Material

The material used for all tests conducted in this investigation was ASTM A106 steel. The specimens were removed from a 39 inch (990 mm) diameter pipe with a 3.75 inch (95 mm) thick wall. The specimens were tested in the L-C orientation. The chemical composition of this steel is presented in Table 1 and typical room temperature mechanical properties are listed in Table 2. A Charpy energy - temperature transion curve produced from specimens oriented in the L-C direction is plotted in Figure 1. All J-integral resistance curve tests were conducted at room temperature which is in the transition region for this steel.

Testing Procedure

The specimens were 1 inch (25 mm) thick 1T compact tension specimens with 20% side grooves as shown in Figure 2. The specimens were fatigue precracked to a nominal initial crack length of $a_o/W = 0.65$. The tests were conducted in a screw-driven test machine with a spring in series which allowed the compliance of the testing machine to be varied between tests, Figure 3. The spring consisted of a pair of 1 inch (25 mm) thick titanium plates separated by a pair of rollers. By changing the span of the rollers, a range of stiffnesses could be achieved; a short span produced a stiff system and a large span produced a relatively compliant loading system. This is the same system used by Joyce and Vassilaros[3], and Vassilaros, et al.[4] in their previous

investigations. The stiffness of the testing machine was varied between 10500 lbs/in (1840 N/mm) and 7400 lbs/in (1300 N/mm).

During the tearing instability tests, load, crack opening displacement, and system compliance were recorded digitally at approximately 0.5 s intervals with an interactive computer system. The crack length was monitored continuously by using the D.C. potential drop technique. High speed digital oscilloscopes were also used to record the load, crack opening displacement, compliance and crack length during the instability event. The data acquisition rate during the instability event was 1 μs per point. The oscilloscopes were triggered by the sudden increase in crack opening displacement which occurred when the crack became unstable. Pre-triggering was used so that data prior to the instability could be matched up with the data taken interactively with the computer.

ANALYSIS PROCEDURE

J integral resistance curves were calculated for each test according to the expression[5]

$$J_I = [J_i + \eta A_{i,i+1}/b_i B_N][1-\gamma(a_{i+1}-a_i)/b_i] \quad (1)$$

where

η	= 2 + (0.522)b_i/W for the compact specimen
W	= Specimen width
γ	= 1 + (0.76)b_i/W
b_i	= instantaneous length of the remaining ligament, (W-a_i)
a_i	= instantaneous crack length
B_N	= minimum specimen thickness
$A_{i,i+1}$	= Area under the load versus load-line displacement record between lines of constant displacement at points i and i+1

The crack length was determined from the D.C. potential drop data and calculated according to the expression[6]

$$a = [(\overline{PD} - 0.605)^{0.345}/1.5]*W \quad (2)$$

where

$\overline{PD} = (PD-P_1)/(P_2-P_1)$
P_1, P_2 = calibration constants

Equation (2) requires a two-point calibration which relates the initial and final crack lengths to the repective potentials. For several of the tests, the instability event led to complete separation of the specimen halves and it was not possible to determine the calibration constants, P_1 and P_2 using this approach. For these cases, a value of $P_1 = 0.2$ was assumed. This is an average value of P_1 calculated from many tests conducted on 1T compact specimens from the same section of A106 steel pipe. It should be noted that this value of P_1 is specific to the instrumentation and procedure employed in this testing program and does not apply in general to other materials or experimental apparatus.

The material tearing modulus was calculated from the expression,

$$T_{material} = (E/\sigma_o^2)(dJ/da) \quad (3)$$

where
E = elastic modulus
σ_o= flow stress $(\sigma_y + \sigma_u)/2$
dJ/da = slope of the J-R curve

dJ/da was calculated from a least-squares power law fit to the J-R curve of the form[7]

$$J = A_1(\Delta a)^{A_2} \quad (4)$$

The applied tearing modulus was calculated using the expression of Ernst, et al.[5]

$$T_{applied} = (E/\sigma_o^2)(dJ/da)$$
$$= (E/\sigma_o^2)\{-\gamma J/b + \eta^2 P/b^2[1/(H'/WH + K_M/P)]\} \quad (5)$$

where

γ = 1 + (0.76)b/W
b = remaining ligament, (W-a)
η = 2 + (0.522)b/W
K_M = machine stiffness
W = specimen width
E = elastic modulus
σ_o = flow stress, $(\sigma y + \sigma u)/2$
$H'/H = (1/P)\ (dP/d\delta) + (\eta^2 P/b^2)[(dJ/da) + \gamma J/b]$
$dP/d\delta$ = slope of the load-load point displacement curve
dJ/da = slope of the material J-R curve

In order to reduce oscillations in the calculation of $T_{applied}$, the load-displacement data was smoothed by averaging the data over 30 point intervals. The smoothing had a negligible effect on the calculation of J, but provided for a great reduction in the oscillations in $T_{applied}$ by providing smoother derivatives in the H'/H function.

RESULTS AND DISCUSSION

A summary of the results for the tests is presented in Table 3. The power law fits to the J-R curves from these tests are plotted in Figure 4. There is a considerable amount of variability in the J-R curves from specimen to specimen that is not normally expected since all of the curves were measured using the same material, specimen geometry and nominal initial crack length. This variablity may be due in part to the location of the specimens in the wall of the pipe or the fact that this material is in transition at the test temperature. The difference in the J-R curves beyond J_{Ic} made it difficult to separate the effect of varying the amount of stable crack growth by changing the system compliance since the material resistance to tearing from specimen to specimen was not consistent.

Table 1. - Chemical Composition of ASTM A106 Steel

	C	S	P	Si	Ni	Mn	Cr	Fe
wt %	0.26	0.017	0.028	0.022	0.26	0.9	0.11	bal

Table 2. - Mechanical Properties of ASTM A106 Steel at Room Temperature

0.2% Yield Strength (ksi)	Ultimate Strength (ksi)	Flow Stress (ksi)	% Elong. (in 1 in.)	Reduct. in Area (%)	J $(in\text{-}lb/in)^2$
50.0	79.0	64.5	31	70	950

Table 3. - Summary of Fracture Test Results

Specimen ID	a/W	Machine Stiffness lbs/in (N/mm)	J at Inst. $in\text{-}lb/in^2$ (kJ/m^2)	Delta a at Inst. in. (mm)	$T_{material}$	$T_{applied}$
GAF-2	0.68	8650 (1514)	3062 (536)	0.107 (2.72)	76	71
GAF-3*	0.65	7850 (1374)	3068 (536)	0.077 (1.96)	125	123
GAF-4	0.65	9750 (1710)	3349 (586)	0.81 (2.04)	151	110
GAF-5*	0.65	7400 (1296)	3363 (590)	0.094 (2.39)	120	85
GAF-6	0.65	10350 (1812)	3178 (550)	0.100 (2.54)	128	127
GAF-12	0.66	10350 (1812)	2813 (490)	0.112 (2.84)	91	84

* Fracture mode converted to cleavage after ductile instability

A typical load-displacement record from specimen GAF-6 is shown in Figure 5. The data beyond the point of instability was recorded on the digital oscilloscope. The value of $T_{material}$ at the point of instability was 107 and $T_{applied}$ was 106, Figure 6. These values are in good agreement at the point of instability, but this was not the case for all of the tests. An example of a test in which instability occurred well before $T_{material}$ was equal to $T_{applied}$ is specimen GAF-4, Figure 7. In this case, $T_{material}$ was 126 at the point of instability and $T_{applied}$ was only 92, which would have predicted a stable response. In most cases, instability occurred when the difference between $T_{applied}$ and $T_{material}$ was on the order of 10%, although $T_{material}$ was always greater than $T_{applied}$ at instability.

Several comments are in order regarding the calculation of $T_{applied}$ using the analysis of Ernst, et al. As can be seen from Figures 6 and 7, the $T_{applied}$ curve is not a smooth function as would be expected. This is due to the calculation of the slope of the load-displacement curve from experimental data. All of the functions that go into the calculation of $T_{applied}$ are smooth functions of the crack length or crack extension with the exception of the slope of the load-displacement curve which is determined from the experimental data. Local instabilities such as the growth and coalescence of voids by "fast shear" and other micro-mechanisms cause small fluctuations in the load which lead to large changes in the calculation of the slope of the load-displacement record when the curve exhibits a "flat" nature as was observed in all tests conducted. In the vicinity of maximum load, the calculation of the slope is strongly influenced by the resolution of the

instrumentation and the noise level present in the signal. The fluctuations in load are on the order of magnitude of the noise level present in the signal and it is not possible to separate the two effects. An additional factor to consider is the system compliance. The spring-in-series used in these experiments exhibited some hysteresis effects as as shown in Figure 8 which is a plot of spring displacement versus applied load. The spring displacement and, hence, the system compliance were calculated under the assumption

$$\delta_{TOTAL} = \delta_{SPRING} + \delta_{LOAD\ LINE} \tag{6}$$

The total system deflection was measured with an LVDT and the spring deflection was calculated using equation (5). In all calculations of $T_{applied}$, the stiffness of the system, K_M, was assumed to remain constant and its value was taken as the slope of the load-spring displacement curve after maximum load since this corresponded to the condition of the system when the instability occurred. (Calculation of the system compliance incrementally over the course of the test produced large oscillations in the $T_{applied}$ curve which would make it difficult to make any conclusions about the applicability of the Ernst analysis.) The hysteresis is probably due to friction between the rollers and the spring plates, although other factors may have contributed as well. The experimental procedure assumed that only one parameter would be varied from test to test, namely, the load train compliance. Since the material behavior was not consistent from specimen to specimen, there were two free variables interacting and it was not possible to conclusively determine the effect of load train compliance on the amount of stable crack growth.

One additional point that has not been addressed is the observation of fracture mode transition during the instability event. In several of the

tests, the fracture mode converted from ductile tearing to cleavage fracture after several hundred mils of crack extension. Figure 9 is a photograph of the fracture surface of specimen GAF-5. In this case the fracture mode converted to cleavage after 0.372 in. (9.4 mm) of ductile tearing. This is important considering the fact that ductile tearing is controlled by both the stress and strain in the vicinity of the crack tip, while cleavage is a stress controlled situation.

CONCLUSIONS

The purpose of this investigation was to evaluate tearing instability theory using experimental techniques which allow constant crack length estimation and therefore an accurate calculation of the applied and material tearing moduli at the point of fracture instability. The applied tearing modulus was varied from test to test using a spring in series with the load train of the testing machine to attempt to produce ductile instabilities at different levels of crack growth.

Two conclusions can be drawn from the results of this investigation. In most cases, fracture instability occurred when the difference between the Ernst $T_{applied}$ formulation and $T_{material}$ was on the order of 10%. The effect of changing the amount of stable crack growth prior to fracture instability by changing the system compliance was obscured due to the sensitivity of $T_{applied}$ in the vicinity of maximum load and material variability in the A106 steel.

It was also observed that the A106 steel specimens exhibited large differences in the resistance curve behavior and that the fracure mode transitioned from ductile tearing to cleavage fracture during the instability event in two of the tests.

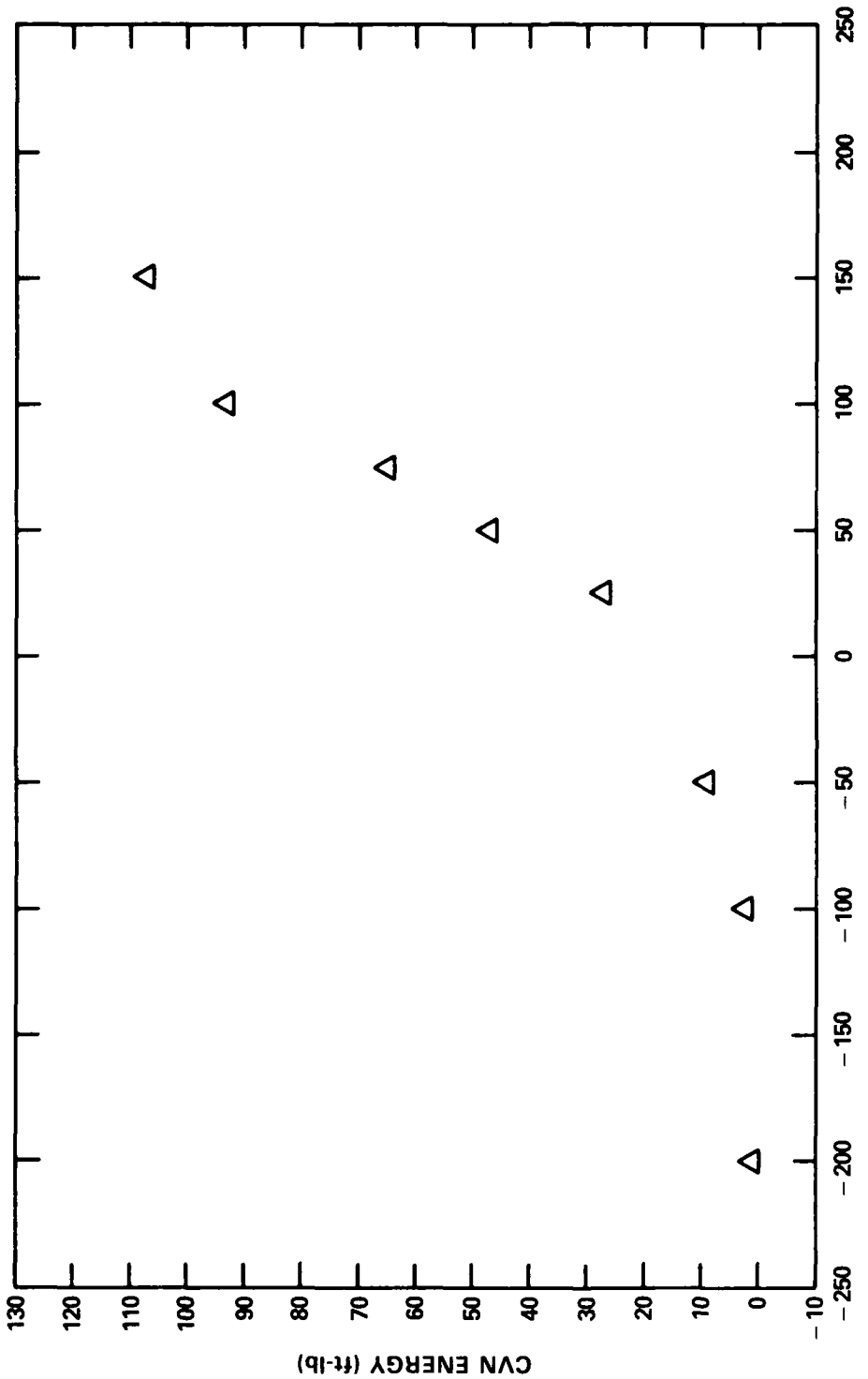

Fig. 1. Charpy energy - temperature transition curve for ASTM A106 steel.

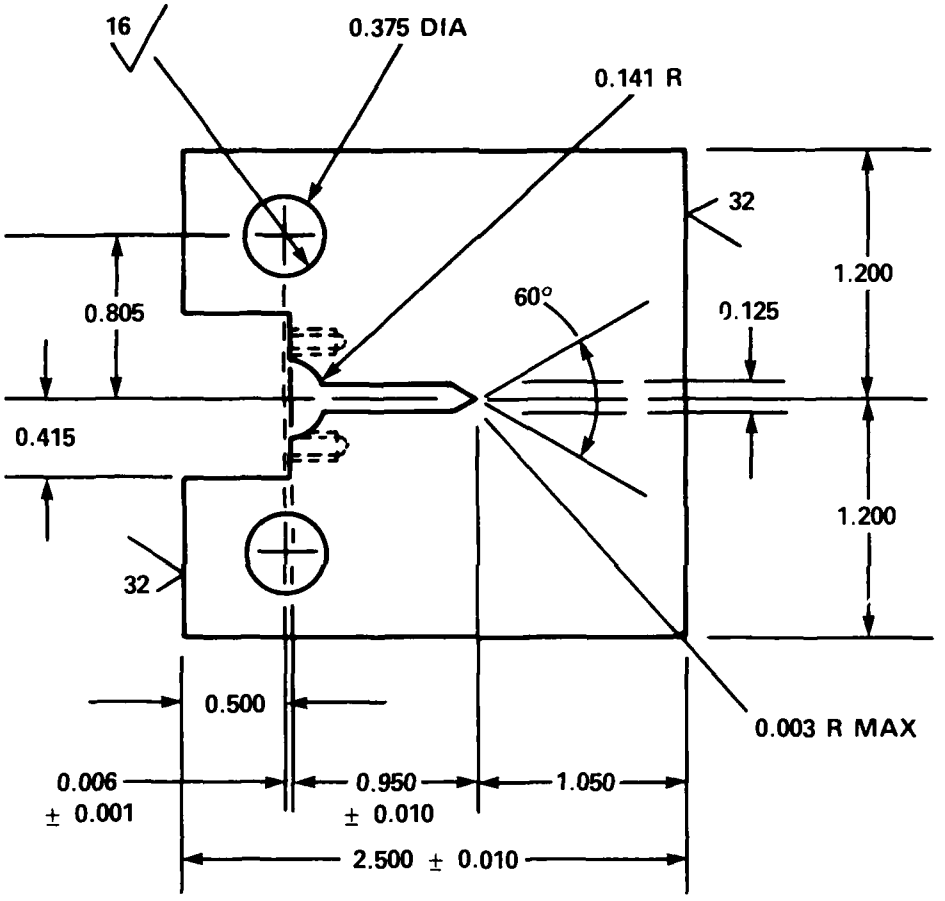

Fig. 2. Modified compact tension specimen drawing.

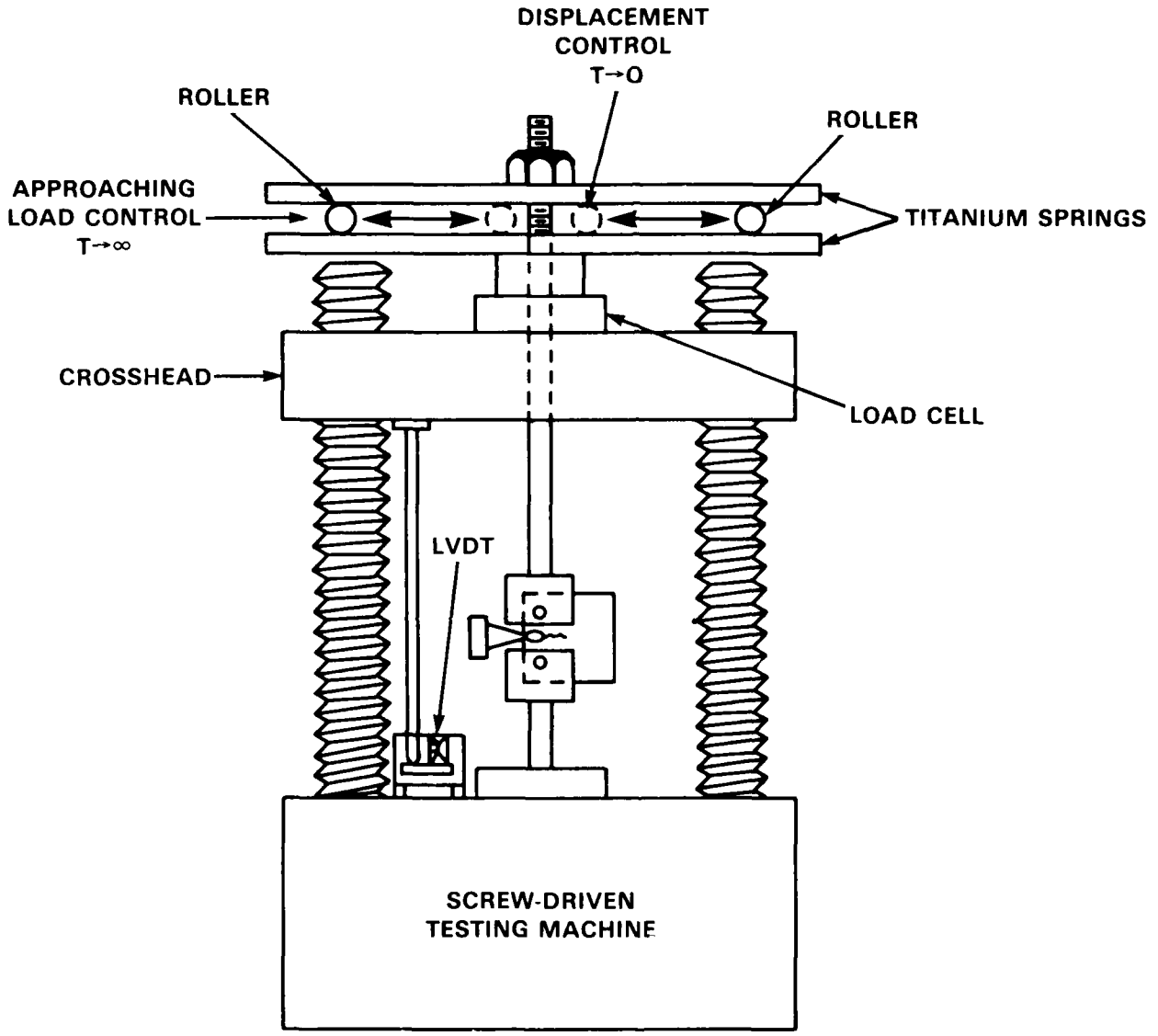

Fig. 3. Schematic of variably compliant test machine arrangement.

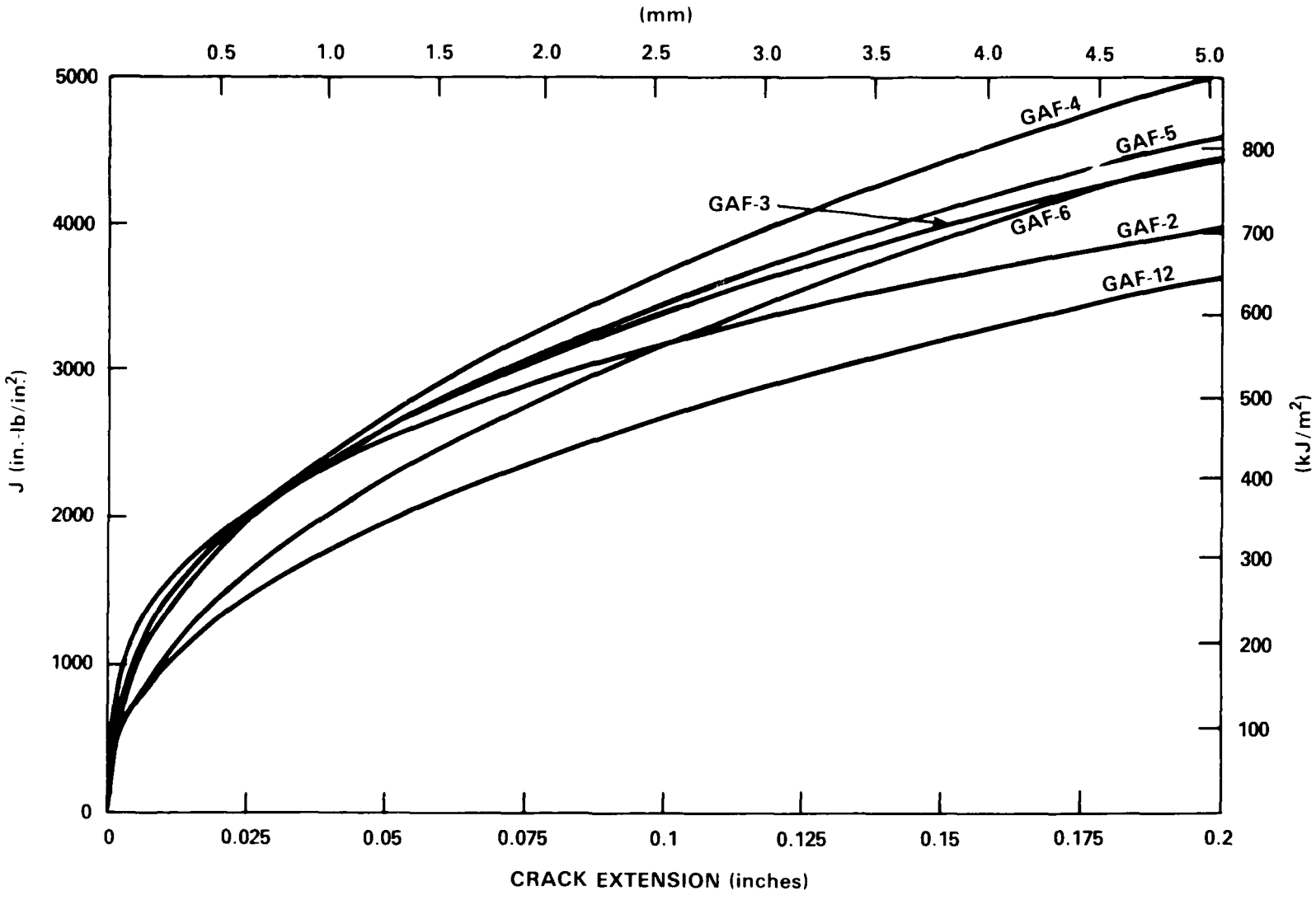

Fig. 4. J-integral resistance curves for 1T compact specimens of ASTM A106 steel.

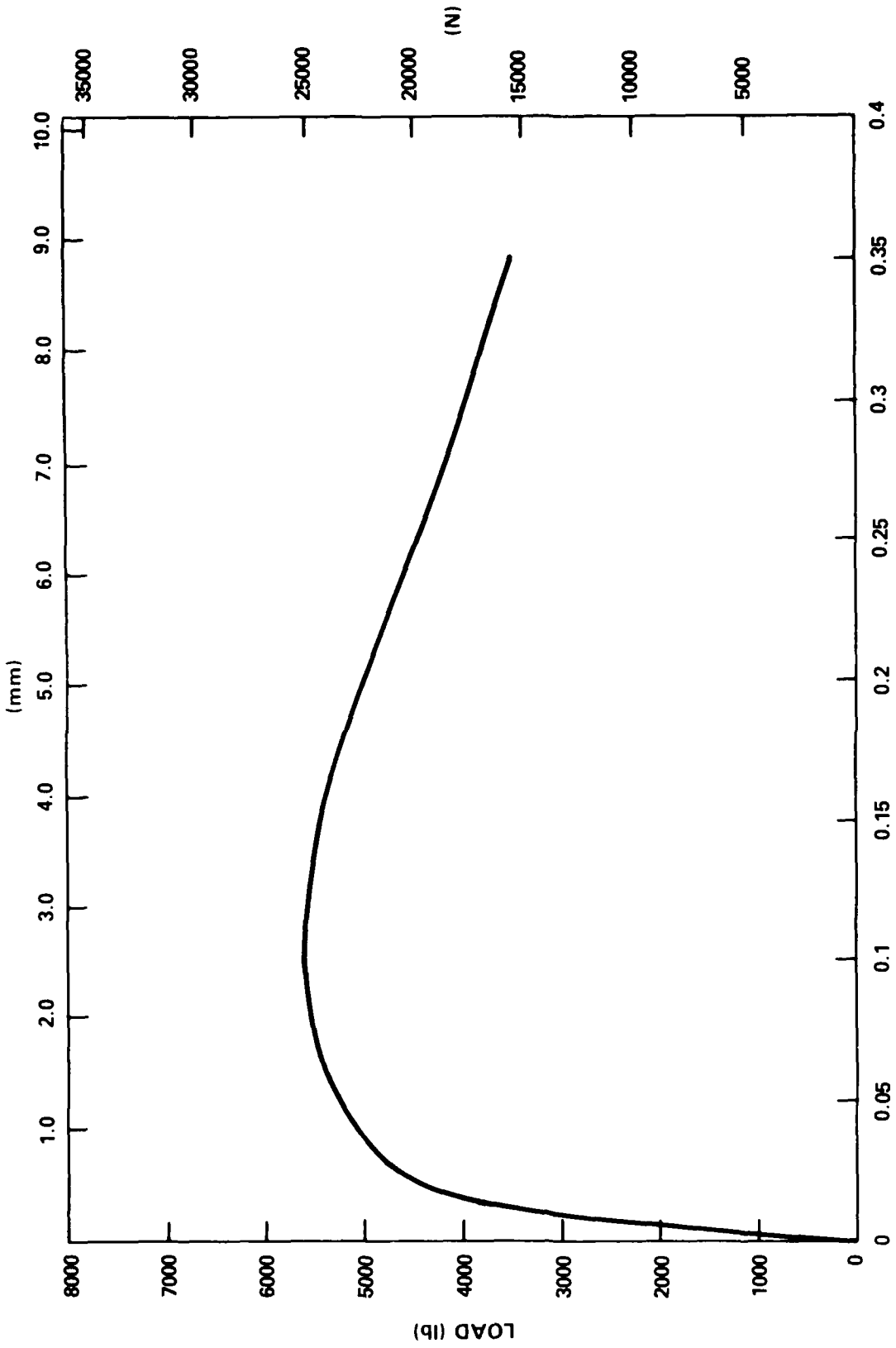

Fig. 5. Load versus displacement record for specimen GAF-6.

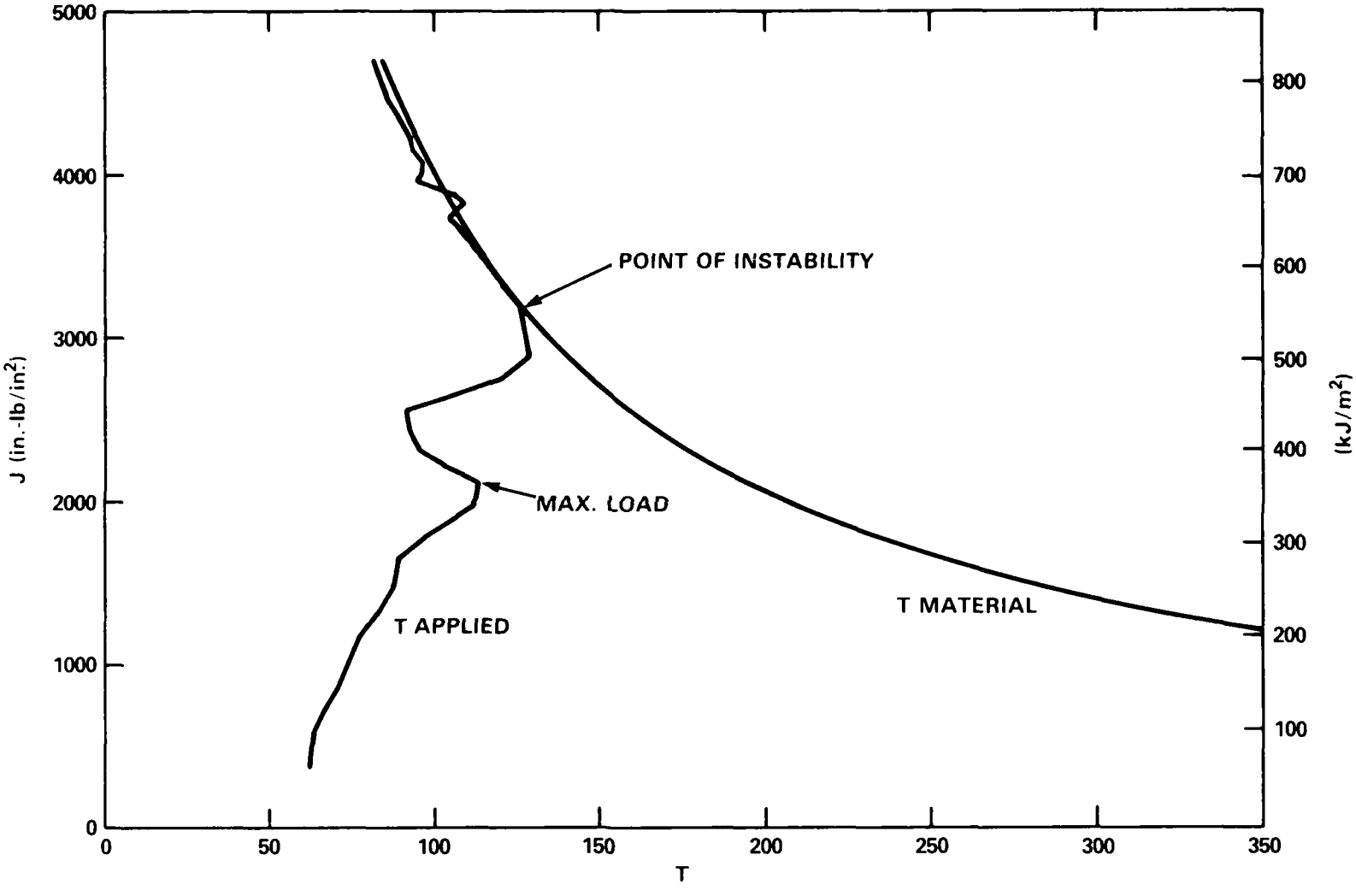

Fig. 6. J versus T plot for specimen GAF-6.

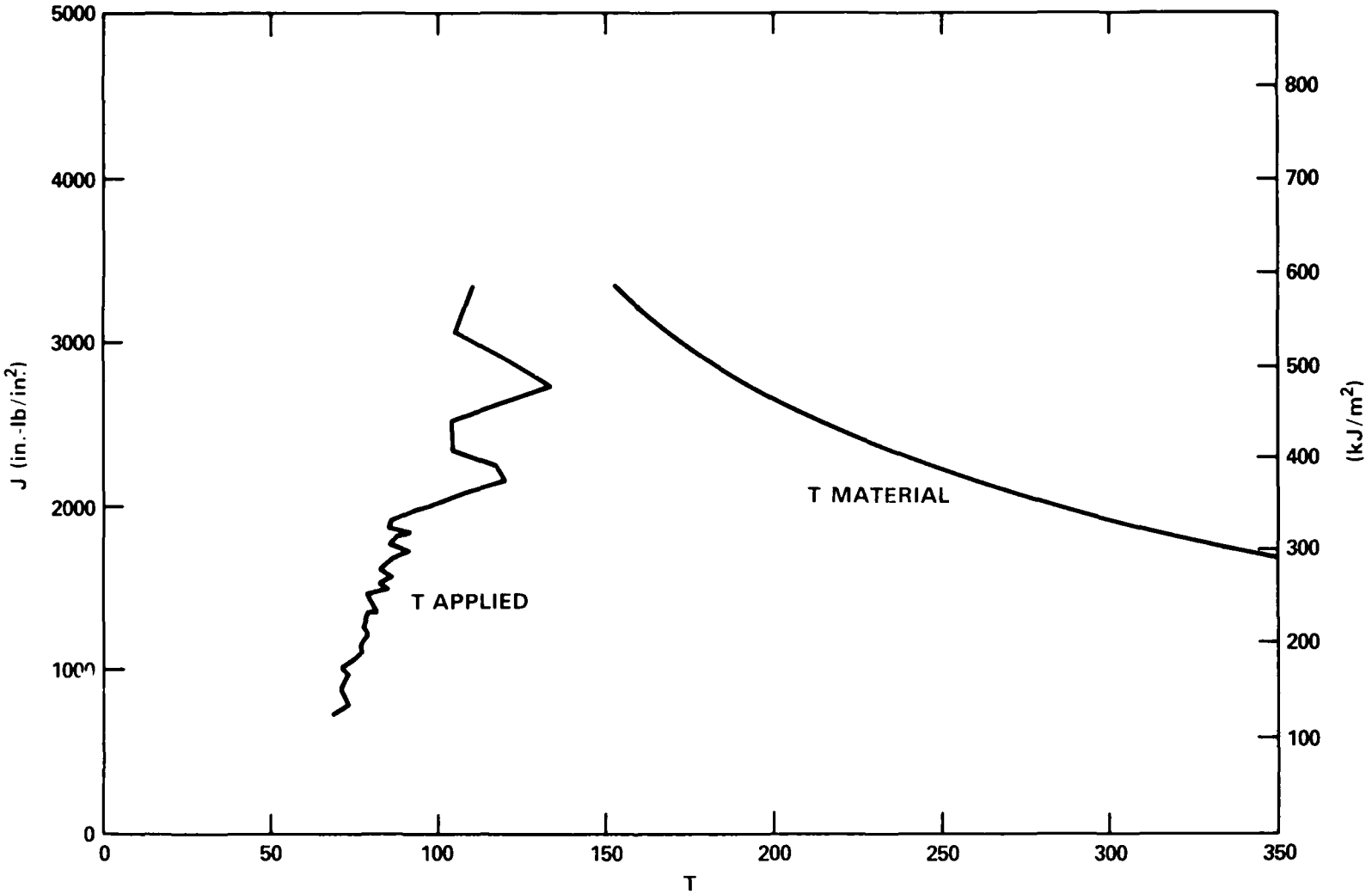

Fig. 7. J versus T plot for specimen GAF-4.

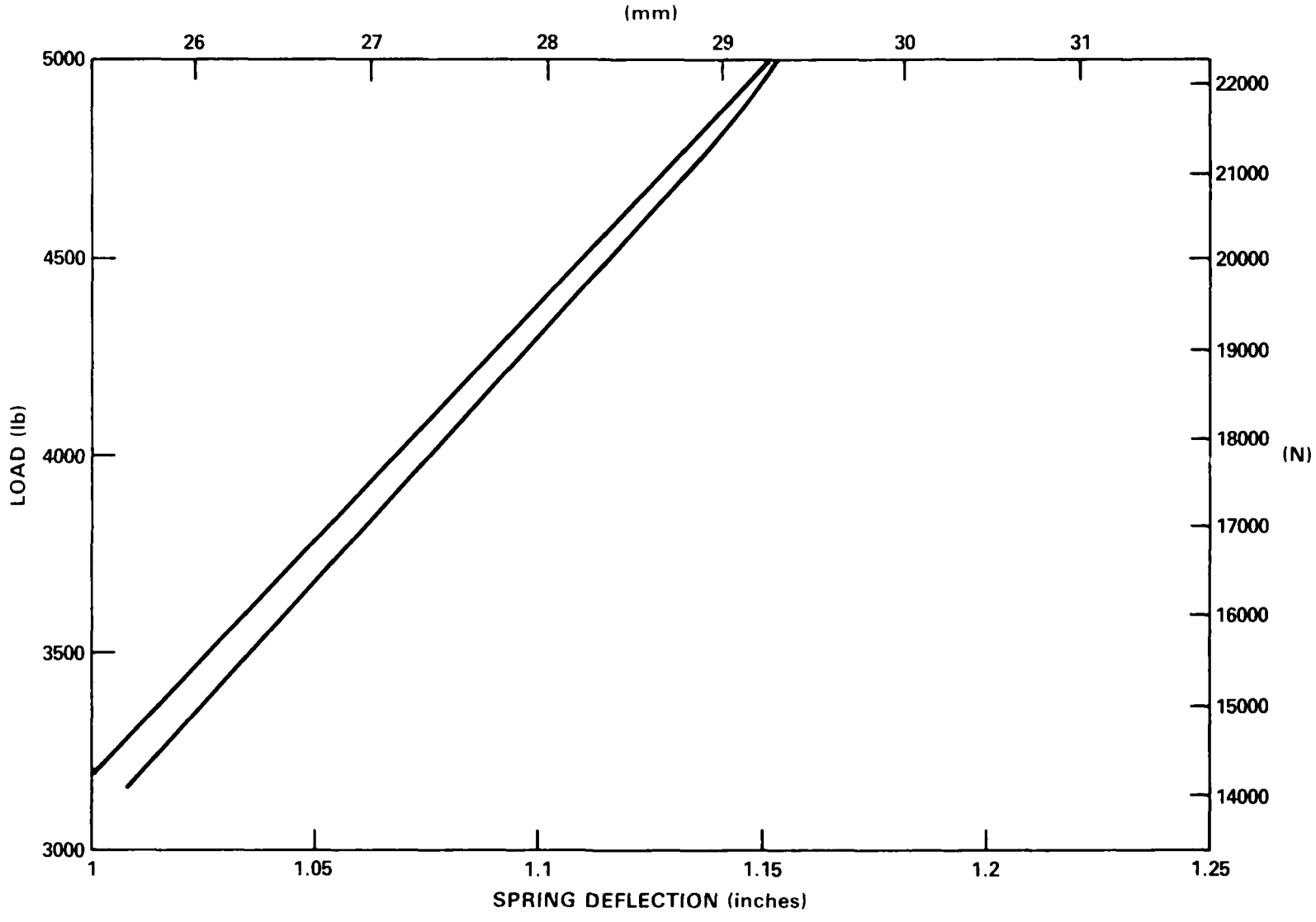

Fig. 8. Load versus spring displacement plot showing stiffness difference between loading and unloading.

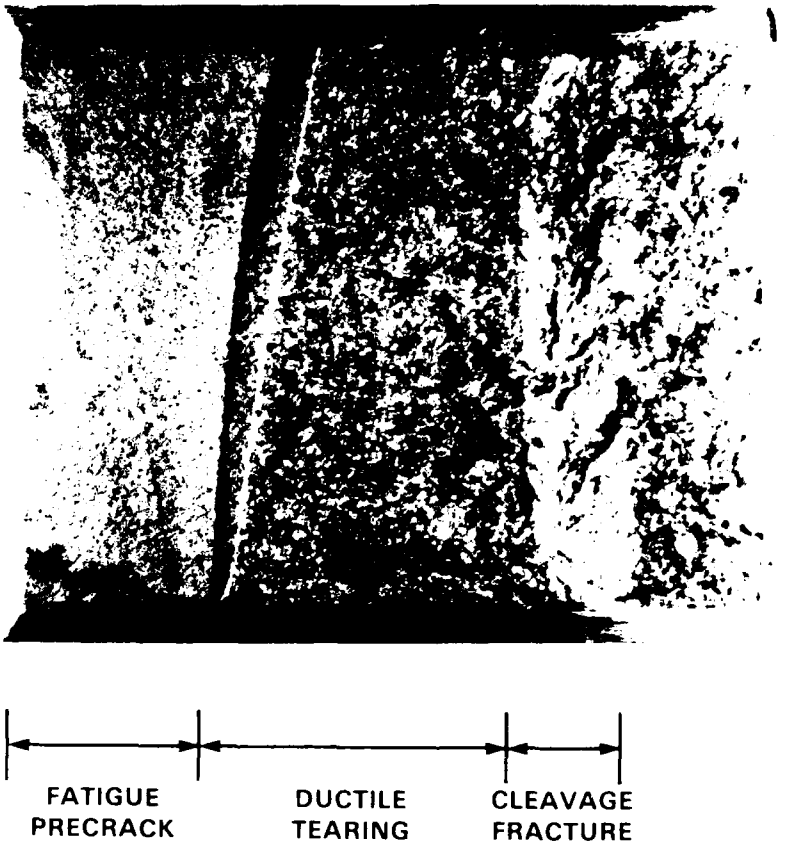

Fig. 9. Photograph of fracture surface for specimen GAF-5 which exhibited ductile fracture to cleavage fracture transition.

REFERENCES

1. Paris, P.C., et al., "The Theory of Instability of the Tearing Mode of Elastic-Plastic Crack Growth," Elastic-Plastic Fracture, ASTM STP 668, pp. 536, (1979).

2. Paris, P.C., et al., "An Initial Experimental Investigation of the Tearing Instability Theory," Elastic-Plastic Fracture, ASTM STP 668, pp. 251-265, (1979).

3. Joyce, J.A., and M.G. Vassilaros, "An Experimental Evaluation of Tearing Instability Using the Compact Specimen," Presented at the Thirteenth National Symposium on Fracture Mechanics, (1980).

4. Vassilaros, M.G., et al., "Experimental Investigation of Tearing Instability Phenomena for Structural Materials," U.S. Nuclear Regulatory Commission NUREG/CR-2570, (1980).

5. Ernst, H.A., et al., "Estimations on J-Integral and Tearing Modulus, T, from a Single Specimen Test Record," Presented at the Thirteenth National Symposium on Fracture Mechanics, (1980).

6. Vassilaros, M.G. and E.M. Hackett, "J-Integral R-Curve Testing of High Strength Steel Utilizing the D.C. Potential Drop Method," ASTM 15th National Symposium on Fracture Mechanics, ASTM STP 833.

7. Carlson, K.W., and J.A. Williams, "A More Basic Approach to the Analysis of Multiple Specimen R-Curves for Determination of J_{Ic}," presented at the Thirteenth National Symposium on Fracture Mechanics, (1980).

INITIAL DISTRIBUTION

Copies		
2	ONR	
	1	1131M
	1	1132SM
4	NRL	
	1	6000
	1	6320
	1	6380
	1	6396
12	NAVSEA	
	1	SEA 05D
	2	SEA 05R
	1	SEA 08
	1	SEA 092
	2	SEA 323
	1	PMS 393
	1	PMS 395
	1	PMS 396
	2	SEA 99612
1	NISC Code 369	
12	DTIC	

CENTER DISTRIBUTION

Copies	Code	Name
1	17	M. Krenzke
1	173	A.B. Stavovy
1	1720.1	T. Tinley
1	28	G. Wacker
1	2802	
1	2803	J. Cavallaro
1	2809	A. Malec
5	281	J. Gudas
10	2814	T. Montemarano
1	522.2	Unclass. Lib.
2	5231	Officer Services

END

4-87

DTIC